ELSEVIER

NeuroImage

www.elsevier.com/locate/ynimg
NeuroImage 28 (2005) 708 – 719

Simultaneous recording of laser-evoked brain potentials and continuous, high-field functional magnetic resonance imaging in humans

G.D. Iannetti,[a,b,*] R.K. Niazy,[b] R.G. Wise,[b] P. Jezzard,[b] J.C.W. Brooks,[a,b] L. Zambreanu,[a,b] W. Vennart,[c] P.M. Matthews,[b] and I. Tracey[a,b]

[a]*Department of Human Anatomy and Genetics, University of Oxford, Oxford, UK*
[b]*Centre for Functional Magnetic Resonance Imaging of the Brain (FMRIB), University of Oxford, Oxford, UK*
[c]*Pfizer UK Ltd., Sandwich, UK*

Received 1 April 2005; revised 15 June 2005; accepted 27 June 2005
Available online 19 August 2005

Simultaneous recording of event-related electroencephalographic (EEG) and functional magnetic resonance imaging (fMRI) responses has the potential to provide information on how the human brain reacts to an external stimulus with unique spatial and temporal resolution. However, in most studies combining the two techniques, the acquisition of functional MR images has been *interleaved* with the recording of evoked potentials. In this study we investigated the feasibility of recording pain-related evoked potentials during *continuous* and *simultaneous* collection of blood oxygen level-dependent (BOLD) functional MR images at 3 T. Brain potentials were elicited by selective stimulation of cutaneous Aδ and C nociceptors using brief radiant laser pulses (laser-evoked potentials, LEPs). MR-induced artifacts on EEG data were removed using a novel algorithm. Latencies, amplitudes, and scalp distribution of LEPs recorded during fMRI were not significantly different from those recorded in a control session outside of the MR scanner using the same equipment and experimental design. Stability tests confirmed that MR-image quality was not impaired by the evoked potential recording, beyond signal loss related to magnetic susceptibility differences local to the electrodes. fMRI results were consistent with our previous studies of brain activity in response to nociceptive stimulation. These results demonstrate the feasibility of recording reliable pain-related LEPs and fMRI responses simultaneously. Because LEPs collected during fMRI and those collected in a control session show remarkable similarity, for many experimental designs the integration of LEP and fMRI data collected in separate, single-modality acquisitions may be appropriate. Truly simultaneous recording of LEPs and fMRI is still desirable in specific experimental conditions, such as single-trial, learning, and pharmacological studies.

Keywords: Nociceptive system; Laser stimulation; Laser-evoked potentials (LEPs); Electroencephalography (EEG); Functional magnetic resonance imaging (fMRI)

Introduction

The simultaneous collection of electroencephalographic (EEG) and functional magnetic resonance imaging (fMRI) data has the potential of providing information on brain activity with unique spatial and temporal resolution.

Scalp EEG detects changes in electrical potentials generated by synchronized synaptic processes in cortical pyramidal cells, and provides a direct measure of spontaneous or stimulus-evoked underlying neuronal activity on a millisecond time-scale (Speckmann and Elger, 1999). However, scalp signals have a rather low spatial definition, because skull and meningeal structures surrounding the brain distort and exert a spatial low-pass filtering on electrical currents, preventing the discrimination between distinct but spatially closed neural sources (Baumgartner, 2004). Furthermore, the spatial localization of the active neural structures responsible for the measured distribution of electromagnetic fields on the scalp relies on the solution of the inverse problem, which provides only inexact solutions and implies an assumption regarding the number and initial location of intracranial generators, modeled as current dipoles (Michel et al., 2004).

In contrast, blood oxygen level-dependent (BOLD) fMRI measures the changes in blood oxygenation, which are linked, though not equivalent, to changes in neuronal activity (Kwong et al., 1992; Ogawa et al., 1992). This technique has excellent spatial resolution in the order of millimeters and does not require any assumption about the number and the location of active neuronal clusters. However, the temporal delay between neural activity and hemodynamic response is on the order of seconds, and the hemodynamic response itself lasts several seconds (Menon and Goodyear, 2001). Consequently, BOLD fMRI is usually unable to unravel neural processes temporally closer than few seconds.

Because of their complementary features, the fusion of data collected with these two techniques is especially attractive, and it could potentially overcome the general trade-off between spatial and temporal resolution which is, to a variable extent, present in all

* Corresponding author. Department of Human Anatomy and Genetics, South Parks Road, OX1 2JQ, Oxford, UK. Fax: +44 1865 282656.
E-mail address: iannetti@fmrib.ox.ac.uk (G.D. Iannetti).
Available online on ScienceDirect (www.sciencedirect.com).

1053-8119/$ - see front matter © 2005 Elsevier Inc. All rights reserved.
doi:10.1016/j.neuroimage.2005.06.060

neuroimaging techniques (Churchland and Sejnowski, 1988). This fusion, however, poses a number of theoretical and practical challenges.

Sampling brain activity using EEG and fMRI at the same time entails important artifacts that are a consequence of reciprocal interferences between the two recording systems (George et al., 2001). Magnetic susceptibility effects and radiofrequency (RF) interaction associated with EEG electrodes and wires cause signal dropouts and geometric distortion on MR images (Bonmassar et al., 2001a). Degradation of image signal-to-noise ratio due to electromagnetic noise emitted by the EEG recording headbox has also been described (Krakow et al., 2000). Whilst, for EEG data, there are two main classes of artifacts: the *pulse* artifact is caused by cardiac pulse-related movements and blood flow effects within the scanner static magnetic field, and the *imaging* artifact is caused by RF and gradient switching during image acquisition. The pulse artifact is regular, has relatively low amplitude, and occurs even when images are not being acquired. In contrast, the imaging artifact is large and obscures the EEG completely (Allen et al., 1998, 2000). For this reason, most of the studies recording evoked potentials and fMRI in the same session have used an interleaved approach, whereby EEG data are collected during gaps in the acquisition of MR images. Nevertheless, interleaving EEG and fMRI has important practical and theoretical limitations, mainly represented by an inefficient sampling of the neural activity and the consequent hemodynamic response, and by a reduction in the flexibility of the stimulus presentation paradigm (Garreffa et al., 2004; Nebel et al., 2005).

In the present study, we attempt recording time-locked EEG responses to laser stimuli (laser-evoked potentials, LEPs) during continuous, high-field fMRI. Brief radiant heat pulses, generated by laser stimulators, selectively excite free nerve endings in superficial skin layers and thus activate Aδ and C fibers (Bromm and Treede, 1984). The EEG brain responses evoked by standard laser stimuli (late LEPs) are related to the activation of type II mechano-heat nociceptors (AMH II units), small-myelinated primary afferents (Aδ), and spinothalamic tract neurons (Bromm and Treede, 1991; Treede et al., 1995). Aδ-related LEPs consist of different components, and their neural generators have been partly localized in dipole-modeling studies of scalp and subdural recordings, and direct intracranial recordings (for review see Garcia-Larrea et al., 2003). The earliest component is a lateralized, relatively small negative wave (N1), mainly generated by the operculoinsular cortex (Frot and Mauguière, 2003; Tarkka and Treede, 1993; Vogel et al., 2003). The largest signal is a vertex negative–positive complex (N2–P2); the negative component (N2) seems to be the result of activation in the bilateral operculoinsular cortices and contralateral primary somatosensory cortex (Ohara et al., 2004; Schlereth et al., 2003; Tarkka and Treede, 1993); the positive component (P2) is mainly generated by the cingulate gyrus (Iannetti et al., 2003; Lenz et al., 1998; Tarkka and Treede, 1993).

Aδ LEPs, investigated in physiological and clinical studies in patients with peripheral or central lesions (Bromm and Treede, 1991; Iannetti et al., 2001; Spiegel et al., 2003), are now considered the best tool for assessing function of nociceptive pathways (Cruccu et al., 2004).

Recently, laser stimulation has also been combined with fMRI recording to investigate the physiology of brain structures involved in processing nociceptive inputs (e.g., Bornhovd et al., 2002; Youell et al., 2004). Laser stimulation has been demonstrated to be reliable and robust in producing brain responses detectable with fMRI, and laser stimulation during fMRI is becoming increasingly used because its physical properties make it suitable for designing experimental paradigms adequate for the investigation of specific physiological features, like somatotopy (Bingel et al., 2004), anticipation of pain (Sawamoto et al., 2000), perceptual coding (Buchel et al., 2002), and lateralization (Bingel et al., 2003).

In pain research, important physiological information can be obtained using experimental designs which involve single-trial analysis, or investigate cognitive or drug modulation of laser-evoked responses. These paradigms require implementation within a single experiment. Therefore, we investigated the feasibility of detecting brain responses to laser stimulation, using EEG and high-field BOLD-fMRI simultaneously. We assessed: (i) the consistency of LEP results, by comparing latency, amplitude and scalp topography of the main LEP components recorded during continuous fMRI with those recorded outside the scanner room using the same stimulation, recording equipment and experimental paradigm; (ii) the quality of BOLD-sensitive MR images collected during the recording of EEG, using specific stability tests; and (iii) the reliability of recording fMRI responses to nociceptive stimulation in the presence of functioning EEG recording equipment.

The details of the algorithm employed to remove the image and pulse artifacts on EEG data are described in a companion paper (Niazy et al., this issue).

Methods

Seven healthy volunteers participated in the study (5 males, 2 females, age range 27–32 years). All subjects gave their informed consent, and the procedure was approved by the local ethics committee.

Laser stimulation

Painful heat stimuli were generated by an infrared neodymium yttrium aluminium perovskite (Nd:YAP) laser (El.En., Florence, Italy, www.elengroup.com) with a wavelength of 1.34 μm; at this wavelength, energy can be easily transmitted using standard glass fibers (Spiegel et al., 2000), a crucial requisite if the laser stimulation has to be delivered in the MR environment. The diameter of the laser beam was set at 6 mm (irradiated area ~28 mm^2) by focussing lenses. An MR-compatible, in-house developed telescopic periscope was used at the end of the fibre optic to facilitate the stimulation of the hand dorsum when the subject was lying in the scanner. Laser pulses produced by Nd:YAP stimulators do not induce damage to the irradiated skin, not even the transient dyschromic spots sometimes produced by widely-used, high-intensity CO2-laser pulses (Cruccu et al., 2003; Iannetti et al., 2003). In previous experiments, we found that Nd:YAP laser pulses of high intensity (up to a 2 J energy directed to a skin area of about 20 mm^2) and short duration are optimal to elicit painful pinprick sensation (Aδ input) and evoke late LEPs after stimulation of different body sites, without inducing damage to the skin (Cruccu et al., 2003; Iannetti et al., 2004).

Experimental paradigm

For each subject, LEPs were recorded in two sessions on different days, using the same recording system and stimulation

paradigm. In one session LEPs were recorded during continuous fMRI at 3 T (fMRI session). In the other session, LEPs were recorded outside the scanner room (control session). The order of sessions was balanced across subjects.

In each session, 60 laser pulses were directed to the skin of the dorsum of the right hand. The onset, duration, and intensity of the laser stimulation were controlled using in-house developed software (LasCo, Laser Control) and, simultaneously with each pulse, a trigger signal was generated by the laser stimulator and recorded in the EEG system for signal averaging, thus eliminating possible timing discrepancies. Timing of the stimulation was pseudo randomly generated according to a Poisson distribution, with an average inter stimulus interval (ISI) of 22.3 s (ranging between 14 and 33 s); this has been demonstrated to be optimal in detecting the BOLD response in event-related fMRI experiments (Donaldson and Buckner, 2001). To avoid nociceptor fatigue or sensitization, the laser beam was slightly moved after each stimulus by an investigator, and stimuli were delivered arhythmically to minimize central habituation. The duration (4 ms) and the energy (2 J) of the laser pulses, as well as the area (~28 mm^2) of the irradiated spot, were kept constant across sessions and subjects. With these parameters, the stimuli elicited a moderately painful, pinprick sensation that the subjects could tolerate across all 60 stimuli. At the end of each session, subjects were asked to rate verbally the perceived sensation on a numerical rating scale ranging from 0 to 100, where 0 was "no pain" and 100 "pain as bad as it could be" (Jensen and Karoly, 2001).

EEG recording

The EEG recording setting was identical in the fMRI and in the control session. Participants wore MR-compatible, laser-safety goggles and were asked to stay awake and relax their muscles. They were also instructed to keep their eyes opened and gaze slightly downwards. In the fMRI session, the subject's head was restrained using a vacuum pillow. Electroencephalogram was recorded with 30 conventional plastic coated Ag/AgCl electrodes fixed on the subject's head by a common plastic EEG cap, according to an extended 10–20 system. Electrode impedance was kept below 5 kΩ. Current-limiting safety resistors (10 kΩ) were applied on each electrode lead close to the electrode itself, to limit the induced current and minimize lead loops (Lemieux et al., 1997). In order to monitor ocular movements or eye-blinks and to discard contaminated trials, electroculographic (EOG) signals were simultaneously recorded from surface electrodes, one placed over the mid-lower eyelid and the other 1 cm lateral to the lateral corner of the orbit. In order to subtract the pulse artifact, electrocardiogram (ECG) was also recorded in the fMRI session. ECG and EOG channels had 100 kΩ current-limiting safety resistors. All cables were twisted and harnessed in a plastic tube, which in the fMRI session was protected and fixed using foam rubber. Using AFz as common reference, EEG data were digitized with an MR-compatible, 22-bit, 32-channel amplifier (SD-MRI, Micromed, Italy) with the following technical characteristics: bandwith 0.15–600 Hz, sampling rate 2,048 Hz, input dynamic range ±26.5 mV (53 mV peak-to-peak). Such high values of sampling rate and dynamic range are required to record linearly the high-amplitude imaging artifact without amplifier saturation. The signals were then transmitted outside the scanner room through an optic fibre, and stored in a personal computer.

fMRI recording

Functional MRI scanning was performed continuously on Varian INOVA MRI system, with a 3-T magnet (Oxford Magnet Technology). A head-only gradient coil (Magnex SGRAD MKIII) was used with a birdcage radiofrequency head coil for pulse transmission and signal reception. A whole-brain gradient-echo, echo-planar imaging sequence was used for functional scans (TE = 30 ms, 24 contiguous 6-mm-thick axial slices, flip angle 87°, in-plane field of view 256 × 192 mm, image matrix 64 × 64) with a repetition time (TR) of 3 s over 460 volumes, corresponding to a total scan time of 23 min. To allow optimal removal of MR-induced artifacts, a trigger signal was generated from the scanner simultaneously with the RF excitation pulse of every slice of each volume, and recorded on the EEG system (Niazy et al., this issue). Furthermore, for each subject, a T1-weighted, high-resolution structural image (70 contiguous 3-mm-thick axial slices, in-plane field of view 256 × 192 mm, matrix 256 × 192) was collected for anatomical overlay of brain activation and registration.

EEG data processing

Removal of MR-induced artifacts

EEG data were imported and all analyses carried out using EEGLAB (www.sccn.ucsd.edu/eeglab), an open-source toolbox running under MATLAB environment (Delorme and Makeig, 2004). Imaging and pulse artifacts present in the EEG data collected in the fMRI session were removed with in-house developed algorithms, the details of which are described in a companion paper (Niazy et al., this issue).

Laser-evoked potentials (LEPs)

Continuous EEG data were first downsampled to 256 Hz and band-pass filtered from 0.5 to 50 Hz. EEG epochs containing the laser stimuli were then extracted using a window analysis time of 2 s (from 500 ms pre-stimulus to 1500 ms post-stimulus). For each epoch, a baseline correction for the data preceding the stimulus by 500 ms was performed. Preliminary analysis of EEG recordings included visual inspection and removal of trials contaminated by artefacts due to eye blinks or gross movements. To identify LEP components, EEG sweeps time-locked to the laser stimulation were averaged. We measured the peak latency and the baseline-to-peak amplitude of the contralateral early response (N1 component) at the temporal electrode contralateral to the stimulated side (T3) against Fz, and the peak latencies and the baseline-to-peak amplitudes of the late negative (N2) and positive (P2) components of the late response at the vertex (Cz) against average reference. To compare scalp distribution of LEPs, isopotential topographical maps were obtained by linear interpolation of the four nearest electrodes, using amplitudes from grand averaged, reference-free LEP data of each session. Trial-to-trial consistency of the main N2–P2 vertex response was qualitatively assessed by sorting single-trial responses vertically in order of occurrence, with signal amplitude colour-coded (Delorme and Makeig, 2004).

Since both LEP values and psychophysical ratings were distributed normally, their differences in the fMRI and control sessions were assessed by calculating paired Student's t tests, using Prism 4.0 (GraphPad, Sorrento Valley, CA, USA). Since the latency values of the P2 components had different variances in the fMRI and control sessions, their difference was assessed by

calculating a t test with Welch's correction. Results are given as mean ± standard deviation.

fMRI data processing

EPI quality

In order to assess the effect of the presence of EEG recording components and of their functioning on the quality of the fMRI data, a number of specific stability tests were performed. These tests were carried out using a well-characterized agar gel spherical phantom, used in our laboratory for daily image quality assurance testing (Jezzard and Clare, 2002). The phantom was 18 cm in diameter and loaded the head RF coil in a similar way to a human head. Five tests were performed under three different experimental conditions. In condition A, continuous EPI data using identical parameters as those for fMRI were collected without any EEG recording equipment present in the scanner room. These data provided the baseline measurement of stability for our system, and replicated our daily quality assurance procedure. In condition B the EEG cap was placed over the phantom with electrodes attached and filled with conductive gel, but these were not connected to the EEG amplifier. In condition C, the electrodes were connected to the EEG amplifier, and recordings were made from the EEG electrodes during fMRI data acquisition. This last condition simulated that in which EEG data would be recorded from human volunteers.

Each run consisted of a gradient-echo echo-planar imaging (EPI) time series acquisition with the following parameters: TR = 3 s, TE = 30 ms, 21 contiguous 5-mm-thick axial slices, in-plane field of view 256 × 256 mm, image matrix 64 × 64, 104 volumes. The first four volumes from each run were discarded in order to exclude non steady-state magnetization effects from the analysis. The remaining 100 volumes collected in each of the four conditions were analyzed for stability using the following five tests:

Test 1: standard deviation of signal time-course. This test assesses the temporal stability of the signal from a large region of interest (ROI). The ROI was constructed by thresholding the images to remove voxels with less that 5% of maximum signal intensity. This masked image region was then further eroded to yield a final ROI containing the central 80% of the phantom image in each slice. The mean signal in the ROI was calculated for each collected volume, it was plotted against time, and the percentage standard deviation of this time-course was calculated. The desired value of percentage standard deviation is below 0.1%.

Test 2: image signal-to-noise ratio. The signal-to-noise ratio of the image was obtained by dividing the average signal in the image ROI (as described above) by the noise (calculated as the standard deviation, within the same ROI, of the difference image of two volumes collected adjacent in time). Expected signal-to-noise ratio should be >250.

Test 3: standard deviation of single-voxel signal time-course. This test assesses the temporal stability of the signal at single voxel level. The standard deviation of the signal time course was first calculated for each voxel of the image, and a statistical map was produced. This map was then divided by the average image intensity (taken from the large ROI mask). Finally, an average value from this percent standard deviation map was calculated within the large ROI. The value of single voxel temporal stability under these conditions should be below 0.5%.

Test 4: ghost artifact. The level of ghosting was calculated and expressed as a percentage of the main image intensity. This should be below 5% of the main image intensity.

Test 5: signal dropout. This test assesses the depth of penetration of the signal dropout artifact caused by the presence of the electrode on the scalp. This was accomplished by first unwarping the geometric distortion in each of the runs using the FUGUE algorithm contained in FSL (FMRIB's Software Library, www.fmrib.ox.ac.uk/fsl). Following removal of geometric distortion the data sets were registered to the data collected in condition A (bare phantom, no EEG components), and then were assessed for unrecoverable signal loss artifact by calculating the depth below each electrode where a signal loss of 25% or greater was observed.

Finally, images were inspected for evidence of image artefacts, both in image- and k-space.

Laser-evoked fMRI responses

Image analysis to reveal significant brain activity based on changes in BOLD signal was performed on each subject's data using FEAT (part of FSL). Prior to statistical analysis, the following processing was applied to each subject's time series of fMRI volumes: motion correction using MCFLIRT (Jenkinson et al., 2002), spatial smoothing using a Gaussian kernel of full width at half maximum 5 mm, subtraction of the mean of each voxel time course from that time course, and nonlinear high-pass temporal filtering (Gaussian-weighted least-squares straight line fitting, with a high-pass filter cut-off of 50 s). The fMRI signal was then linearly modeled (Worsley and Friston, 1995) on a voxel-by-voxel basis using a general linear model approach, with local autocorrelation correction (Woolrich et al., 2001). The results of single-subject statistical analyses were combined in a group analysis carried out using OLS (ordinary least squares) simple mixed effects, thus generating group-representative statistical maps of brain activity in response to nociceptive laser stimulation. For the purpose of such a group-level analysis, registration of low-resolution functional images to high-resolution structural scans was performed for each subject using FLIRT (Jenkinson and Smith, 2001), followed by registration to a standard brain (Montreal Neurological Institute template, Collins et al., 1994). This procedure placed individual subjects' functional image datasets into a common stereotactic space. The raw Z statistic images from the group analysis were thresholded at Z scores greater than 2.5. For each resulting cluster of spatially connected voxels surviving this Z threshold, a cluster probability threshold of $P = 0.01$ was applied to the computed significance of that cluster. The cluster-based significance thresholding at $P = 0.01$ provides a correction for the problem of multiple comparisons (Forman et al., 1995; Worsley et al., 1992).

Results

Quality and intensity of sensation

Laser stimuli elicited a clear pinprick sensation in all subjects. The average pain ratings to laser stimuli were 36 ± 14 in the fMRI

session and 39 ± 17 in the control session, and were not significantly different ($P > 0.20$, paired t test).

Laser-evoked potentials (LEPs)

Nd:YAP laser stimulation of hand dorsum during continuous fMRI evoked clear and reproducible time-locked Aδ-LEPs. Fig. 1 shows the grand mean LEP waveforms and scalp maps obtained during fMRI and in the control session. Examining the grand mean of both sessions, the earliest identifiable response was the negative component (N1) visible in EEG data recorded from the temporal electrode contralateral to the stimulated side (Tc). The N1 waveform was similar in the two sessions; its latency and amplitude were 164 ms and 1.5 μV in the fMRI session and 163 ms and 2.9 μV in the control session. The N1 component was followed by the main negative (N2) and positive (P2) components, both with a scalp maximum in the midline near the vertex. Latencies and amplitudes of N2 and P2 components, as well as scalp maps at the corresponding peak latencies, were remarkably similar in the fMRI and control sessions (N2—fMRI: 208 ms, 8.8 μV; N2—control: 215 ms, 7.8 μV; P2—fMRI 338 ms, 8 μV; P2—control: 351 ms, 8.1 μV) (Fig. 1).

In all subjects, laser stimulation evoked clear vertex N2 and P2 components in both sessions. One subject did not yield a clear N1 component in both sessions, and another subject did not yield a clear N1 component in the fMRI session only. Paired comparisons of all measured LEP data did not disclose any significant difference between fMRI and control sessions ($P > 0.20$; t test, Table 1). Trial-to-trial consistency of the main N2–P2 vertex response was also remarkably similar in the two sessions, as qualitatively assessed by sorting single-trial responses vertically in order of occurrence, with signal amplitude colour-coded (Fig. 2).

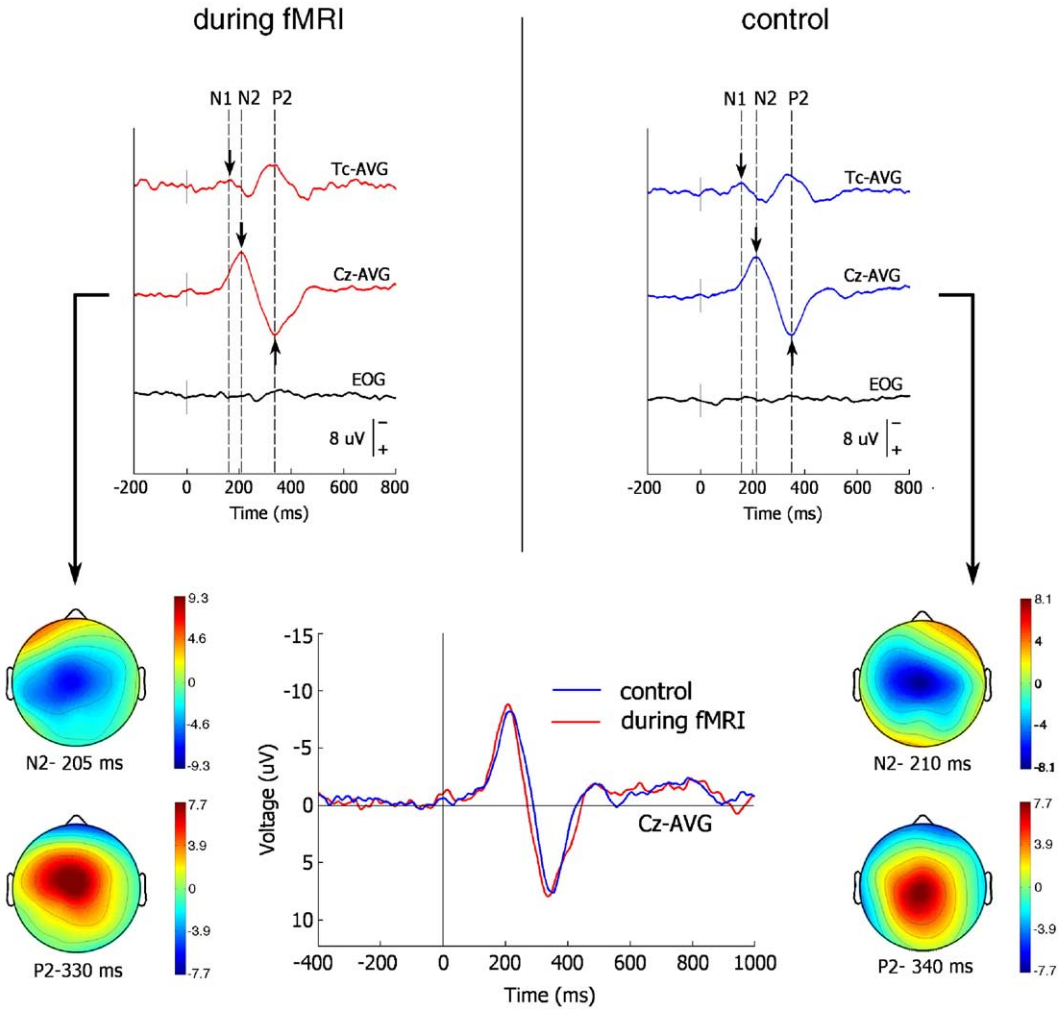

Fig. 1. Laser-evoked potentials (LEPs) recorded during fMRI. Comparison between waveforms and scalp topography of LEPs recorded during continuous fMRI at 3 T (left panel) and in the control session outside the scanner room (right panel), using the same recording equipment and experimental paradigm. Grand averages from the same 7 subjects, after stimulation of the right hand. Negativity is plotted upward. Recordings from the vertex (Cz) and the temporal electrode contralateral to the stimulated side (Tc) are computed against average reference (AVG). Electro-oculogram (EOG) was recorded to monitor eye-blinks and discard contaminated trials. Arrows indicate early N1 and late N2–P2 components. Scalp topographies are shown at N2 and P2 peak latencies. Note the similarity between scalp maps obtained during fMRI and in the control session, as well as the equivalence between latencies and amplitudes of N2 and P2 vertex components, as shown in the superimposed grand averages (lower panel).

Table 1
Laser-evoked potentials (LEPs) and perceived intensity obtained during fMRI and in a control session in 7 normal subjects

Experimental session	N1 component[a]		N2 component[b]		P2 component[b]		Perceived intensity (0–100)
	Latency (ms)	Amplitude (μV)	Latency (ms)	Amplitude (μV)	Latency (ms)	Amplitude (μV)	
fMRI	162 ± 7 (152–167)	3.3 ± 2.1 (1.1–6)	214 ± 17 (201–243)	10.5 ± 5.4 (4.1–19.7)	343 ± 26 (301–382)	8.9 ± 3.2 (6.1–13.1)	39 ± 17 (19–68)
Control	163 ± 11 (152–174)	4.1 ± 3.6 (0.9–8.2)	215 ± 14 (199–233)	8 ± 1.2 (6.9–9.7)	352 ± 6 (344–360)	8.1 ± 1.8 (6.2–10.1)	36 ± 14 (23–62)
Difference	ns	ns	ns	ns	ns[c]	ns	ns

Mean ± standard deviation (range).
ns = not significant (paired t test, $P > 0.20$).
[a] Recorded from the contralateral temporal electrode (T3) against Fz.
[b] Recorded from Cz against average reference.
[c] t test with Welch's correction.

Quality of MR images

Test 1: standard deviation of signal time-course

The left graph in Fig. 3 shows the results of the analysis of temporal standard deviation in a large ROI. In a stable system with no sources of interference, this value indicates the stability of the radio-frequency amplifier used for RF pulse transmission. As shown in the graph, no indication of compromised stability was observed, with the percentage standard deviation for each condition being below the desired value of 0.1%, and with no statistically significant differences in the stability between conditions. The error bars in each graph represent the variability (standard deviation) of results across the 21 slices analyzed.

Test 2: image signal-to-noise ratio

The results for image signal-to-noise ratio are plotted in the right graph of Fig. 3. No significant difference in signal-to-noise ratio was observed between condition C (simulating EEG acquisition) and condition A (phantom without EEG equipment).

Test 3: standard deviation of single-voxel signal time-course

Fig. 4 shows the results of the assessment of voxel-by-voxel standard deviation within the image ROI. Again, these data show that there was no significant difference between conditions C (simulating EEG acquisition) and A (phantom without EEG equipment).

Test 4: ghost artifact

The analysis of the level of EPI ghosting in the images showed a stable level of ghosting across slices and across runs of 4 ± 2%.

Test 5: signal dropout

Analysis of the signal dropout artifact caused by the magnetic field distortions surrounding the electrodes revealed an observable effect in our 3 T gradient-echo EPI data. The average depth of affected signal (depth within which a 25% or greater signal dropout was observed) was calculated to be between 4 mm and 8 mm in the vicinity of each electrode. This level of signal loss was seen in each of the 2 conditions (B and C) when the electrodes were attached to the phantom.

The final inspection of the data for signs of interference or other artifacts did not reveal any further unwanted features.

Laser-evoked fMRI responses

Group analysis of fMRI data collected continuously during the LEP recording revealed a network of brain regions activated in response to laser stimulation (Fig. 5). Cortical and subcortical regions including the bilateral thalamus, the peri-acqueductal gray, the bilateral insular cortex, the anterior cingulate cortex, the bilateral secondary somatosensory cortex (SII) and the contralateral sensorimotor cortex showed significant activation in response to laser stimulation ($Z > 2.5$ and activated cluster significance $P < 0.01$). This pattern of activity is consistent with previous reports of nociceptive-related brain activity (Jones et al., 1991; Peyron et al., 2000; Tracey et al., 2002).

Discussion

In this study we demonstrate that brain responses to selective laser stimulation of nociceptive afferents can be detected by recording EEG and fMRI simultaneously.

The quality of EEG signals collected during continuous fMRI is sufficient to record LEPs with latencies, amplitudes, and scalp distribution similar to control recordings. BOLD-fMRI images acquired during LEP recording were not affected by the presence of the functioning recording equipment, and the fMRI responses to laser stimulation were consistent with the common patterns of brain activity in response to nociceptive stimulation.

Afferent input and EEG brain responses

To study the physiology of sensory systems, the availability of a stimulus able to activate the system under investigation in a robust, highly controllable and selective way is a crucial requirement. In addition, when the temporal characteristics of the underlying brain processing need to be explored (e.g. recording stimulus-evoked EEG responses), the stimulus has to be very short, to elicit a sensory volley sufficiently synchronized to allow the recording of time locked brain responses using EEG or MEG. In pain research, solid-state (YAG/YAP) lasers fulfil these requisites, eliciting reliable pain-related EEG brain responses (LEPs), selectively related to the activation of AMH II nociceptors (Cruccu et al., 2003; Iannetti et al., 2004; Iannetti et al., 2005). Compared with CO2 lasers, solid-state lasers emit a radiation with a much shorter wavelength (1–2 μm), and consequently their radiation penetrates deeper and the energy is dispersed over a larger skin volume. As a consequence, the heat is directly absorbed at the nociceptor depth (approximately

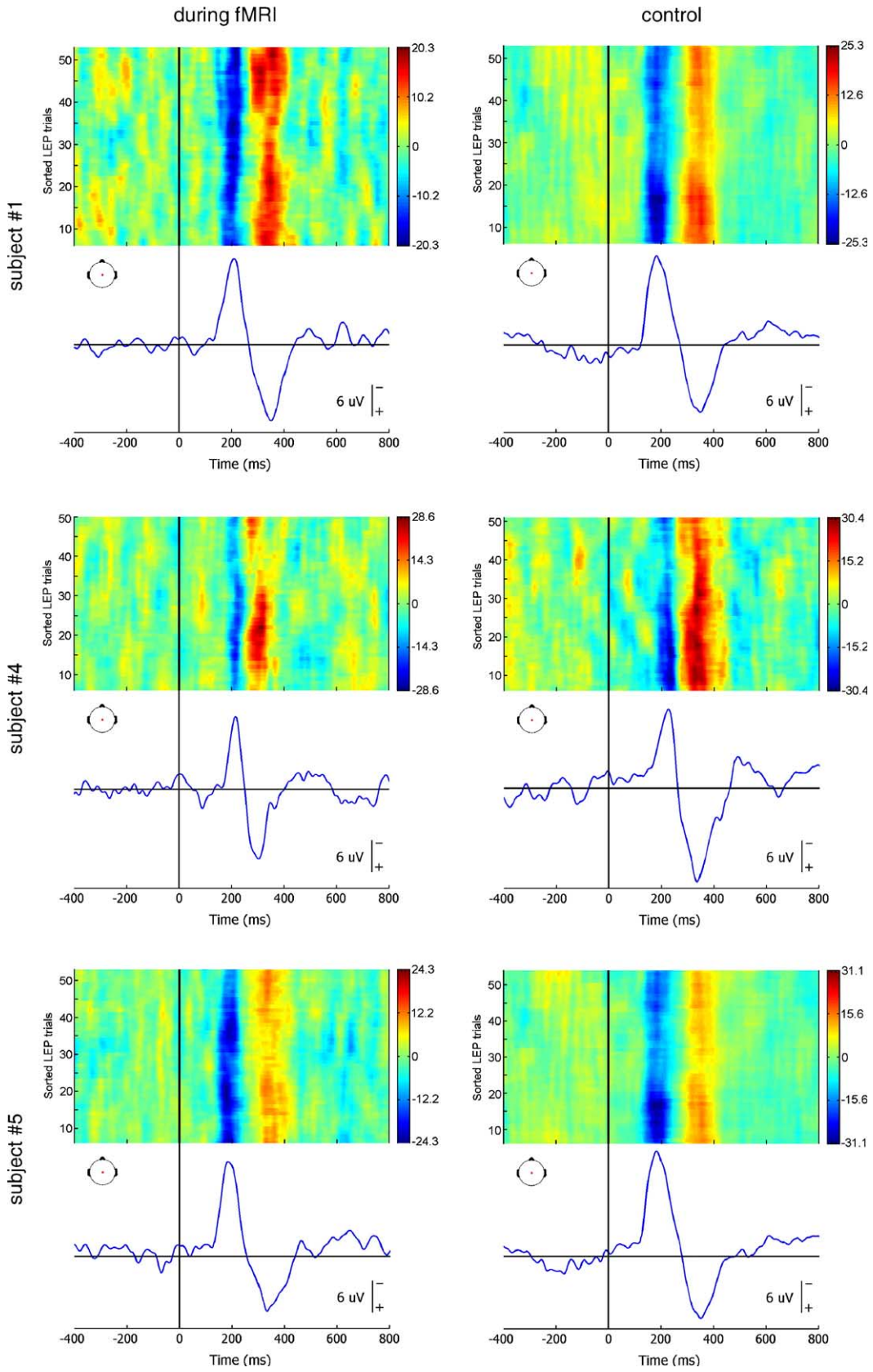
during fMRI
control
subject #1
subject #4
subject #5
Sorted LEP trials
Time (ms)
6 uV
20.3
10.2
0
-10.2
-20.3
25.3
12.6
-12.6
-25.3
28.6
14.3
-14.3
-28.6
30.4
15.2
-15.2
-30.4
24.3
12.2
-12.2
-24.3
31.1
15.6
-15.6
-31.1

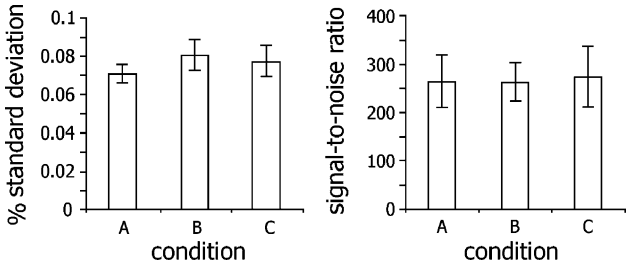

Fig. 3. Stability of echo-planar images (EPIs) collected during EEG recording. The graphs show the results of two different stability tests performed in three different experimental conditions. In condition A, pseudo fMRI data were collected on a phantom without the EEG recording equipment in the scanner room. In condition B the EEG cap with electrodes and conductive gel was placed over the phantom, but the electrodes were not connected to the EEG amplifier. In condition C, the electrodes were connected to the EEG amplifier, and recordings were made from the EEG electrodes during fMRI data acquisition, thus simulating the conditions under which EEG data were recorded from human volunteers. The left graph shows the results of the test which assesses the temporal stability of the signal time-course from a large region of interest (ROI), by calculating the percentage standard deviation in the signal time course (desired values are below 0.1%); *y* axis: percentage standard deviation; *x* axis: experimental condition. The right graph shows the results of the test which assesses the image signal-to-noise ratio, by dividing the average signal in the large ROI by the standard deviation within the same ROI applied to the difference image of two image volumes adjacent in time; *y* axis: signal-to-noise ratio; *x* axis: experimental condition. The error bars in each graph represent the variability (SD) of results across the 21 slices analyzed. Details of the ROI definition are reported in Methods.

200 μm), and nociceptive afferents are activated more rapidly and mostly directly (Spiegel et al., 2000). In addition, the high energy density of laser emission allows stimulus durations in the order of milliseconds, and the resulting activation of afferent nerve fibers is thus also highly coherent (Iannetti et al., 2004). For these reasons, solid-state laser stimulation yields a highly synchronized afferent volley, which provides a stronger and selective nociceptive input to the brain (Baumgärtner et al., 2005).

Raw EEG data recorded during MRI scanning includes major artifacts and must undergo several additional processing steps which introduce the risk of signal degradation. In this study, we used a solid-state Nd:YAP laser stimulator because it allowed us to deal with EEG responses with maximal signal-to-noise ratio and hence more resistant to possible signal degradation by optimizing the quality of the temporal features of the somatosensory input (Iannetti et al., 2004).

Our results show that LEPs can be recorded reliably during continuous fMRI, and that the processing of raw EEG signal does not significantly affect the quality of the stimulus-evoked responses (Figs. 1, 2). When LEP waveforms from the fMRI session were compared with those from the control session, the latency of the components constituting the main N2–P2 vertex complex was extremely similar (Table 1). While the peak latency of a time-locked response is less sensitive to the quality of the ongoing EEG, the amplitude is more susceptible to noise in the data, especially when the number of trials is relatively low, and more important size differences in response amplitude could have been expected. However, the amplitudes of the N2 and P2 vertex components were remarkably well matched between the fMRI and the control session (Table 1).

Among all the explored LEP values, the only one which showed a noticeable (although non-significant) reduction in the fMRI session (both in grand mean and single-subject data) was the amplitude of the early-latency N1 component (mean, 25% reduction, see Table 1). At least two factors could explain this dissociation between the behavior of N1 and that of N2 and P2 during the fMRI session. Possibly most important is the lower signal-to-noise ratio of the N1 component, which makes it certainly more sensitive to the degradation introduced by the processing of signals recorded in the fMRI session. In addition, a stronger and tonic EMG activity from the *temporalis* muscle could have been recorded selectively in the temporal electrodes during the fMRI session. In fact, the increased sensory input produced by the noise and the vibration of the working scanner, and the increased level of anxiety due to the fMRI experimental setup (where the head position is physically constrained) are factors known to increase the cortical facilitation on interneurons and motoneurons, thus enhancing the tonic background EMG activity. Moreover, visual inspection of the pre-stimulus EEG signals in temporal electrodes suggests increased high-frequency activity when recordings of fMRI sessions are compared to control recordings (data not shown). Because less affected by noise in the data, the latency of N1 was comparable in LEPs recorded in the fMRI and in the control session (Table 1, Fig. 1).

Compared to studies in which single EEG events need to be identified simultaneously with the collection of fMRI data (e.g. detection of interictal spikes in epileptic patients (Lemieux et al., 2001) or of switches between different sleep stages (Czisch et al., 2004)), the averaging technique applied to the evoked potential recognition can help in overcoming some of the difficulties linked to the recording of EEG and fMRI at the same time. If stimulus presentation is jittered in time in respect to the occurrence of the main causes of EEG artifact during fMRI recording (i.e., volume acquisition time and cardiac cycle), possible residuals of imaging and pulse artifacts are treated as background noise and cancelled out during the stimulus-locked averaging procedure. However, standard averaging techniques also can hide important physiological information, and the ability of disclosing responses to single events would allow additional analytical approaches. Single-trial plots of N2–P2 vertex responses in our simultaneous EEG/fMRI data are similar to those observed in the control sessions (Fig. 2), suggesting the feasibility of an analytical approach on a single-event basis. This would permit the assessment of between-trial variations of electrophysiological responses and their relationship with other parameters (e.g., stimulus intensity, psychophysical and fMRI responses), increase the power of statistical analysis and allow within-subject comparisons. In addition, in pain research, the

Fig. 2. Reproducibility of single-trial LEP responses during fMRI. LEPs were collected during continuous fMRI at 3 T (left column) and in the control session outside the scanner room (right column), using the same recording equipment and experimental paradigm. Recordings from the vertex (Cz) in three representative subjects, showing the N2 and P2 components. Each row represents one subject. To emphasize the high trial-to-trial consistency, one bidimensional plot of single-trial responses is shown for each session of each subject. Horizontal lines in the plot represent single-trial responses, with signal amplitude colour-coded at each time point. Responses are sorted vertically in order of occurrence, from bottom (first trial) to top (last trial). The waveform below each plot is the average of all responses. Negativity is plotted upward. Note that single trial responses have considerably higher amplitude than the averaged response, mostly because the latency jitter between trials causes the averaging of signals in opposing phase.

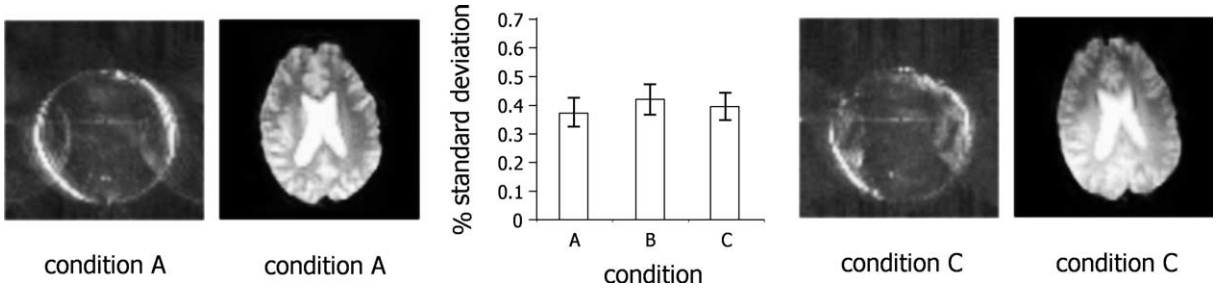

Fig. 4. Single-voxel stability of echo-planar images (EPIs) collected during EEG recording. Same conditions as Fig. 3. This figure shows the results of the test which assesses the temporal stability of the signal time course at single-voxel level. A statistical map where each voxel represents the standard deviation of its signal time course was first calculated, then this map was divided by the average image intensity (taken from the same ROI of the other tests), and finally an average value from this percent standard deviation map was calculated within the large ROI. Percentage standard deviation maps for conditions A (bare phantom, no EEG equipment) and C (phantom with recording EEG equipment) are shown. EPIs collected from one subject in similar conditions (A, no EEG equipment; C: recording EEG equipment) are shown for comparison. Average data are plotted in the graph; *y* axis: percentage standard deviation; *x* axis: experimental condition. The error bars represent the variability (SD) of results across the 21 slices analyzed. Details of the ROI definition are reported in Methods.

use of a single-trial analysis approach is further suggested by the characteristic physiological variability of amplitude and latency of single pain-related neural responses (Carmon et al., 1980; Iannetti et al., 2005; Towell and Boyd, 1993).

Quality of MR images and fMRI brain responses

Collection of MR images in the presence of a functioning EEG recording system is associated with several technical problems, especially when high field echo-planar imaging is performed. Magnetic susceptibility effects and eddy currents associated with EEG electrodes and wires cause signal dropout and geometric distortion (Bonmassar et al., 2001a). Reduction in image signal-to-noise ratio occurs if the electromagnetic noise emitted by the EEG recording headbox is not properly shielded (Krakow et al., 2000). In order to assess the quality of EPI images in the presence of functioning EEG recording equipment, we performed a number of specific and standardized stability tests. The observed results (Figs. 3, 4) indicate that no detrimental effects were introduced into the fMRI data quality by the addition of the functioning EEG recording equipment, beyond the expected effects of signal loss in the immediate vicinity of the electrodes. The size of the observed signal dropouts (4–8 mm) is consistent with what was previously reported on gradient-echo weighted EPIs collected at 1.5 and 3.0 T in the presence of Ag/AgCl electrodes (Bonmassar et al., 2001a; Krakow et al., 2000). In human data acquisitions such effects do not compromise the MR signal from the cortex, because in adult subjects the distance between cerebral cortex and scalp surface is higher than 10–15 mm, and in a dedicated measurement of scalp-cortex distance in 10 normal subjects the smallest individual reported value was 7.5 mm in the temporal region (Krakow et al., 2000). Accordingly, the observed fMRI responses to Nd:YAP laser stimulation were consistent with previous reports of brain activity during processing of nociceptive stimuli (Jones et al., 1991; Peyron et al., 2000; Tracey et al., 2002). Importantly, all the brain structures known to generate scalp LEP components (for review see Garcia-Larrea et al., 2003) showed significant activation in the fMRI data.

Advantages and caveats of simultaneous fMRI/EEG recording

Collecting EEG and fMRI at the same time is challenging. The experimental setup is difficult, and issues related to subject safety and quality of collected data must be addressed using dedicated EEG hardware. Optimal removal of MR-induced artifacts on EEG data requires a complex and time-demanding processing. EEG data processing restrictions and subject's discomfort limit the length of the experimental session and reduce the flexibility of the experimental design. For all these reasons, repeating the same experimental paradigm in separate, single-modality experiments is

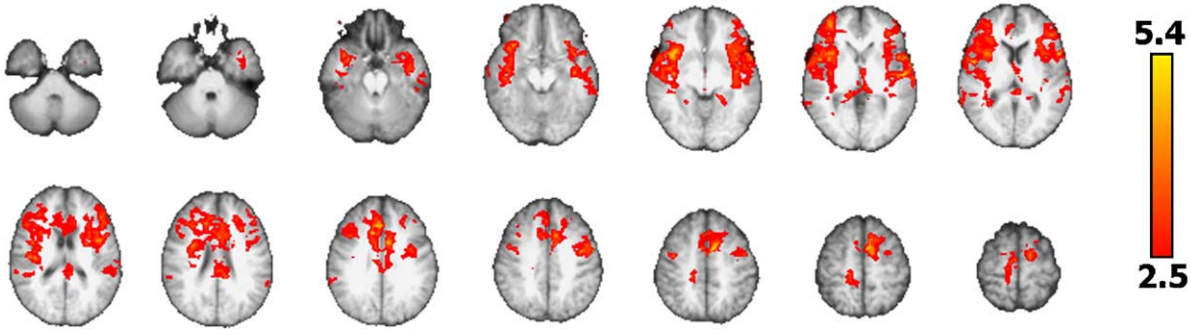

Fig. 5. Laser-evoked fMRI brain responses recorded during EEG. Random effect group analysis, voxel threshold $Z = 2.5$ and cluster threshold $P = 0.01$. The background gray-scale image is the mean structural scan after each scan was coregistered to the standard MNI brain. Brain structures known to generate scalp LEP components show significant activation in the fMRI data. Slices are displayed in radiological convention (right is left, left is right).

a practical strategy for multi-modal studies, and several researchers are focussing on different approaches to combine EEG and fMRI data collected separately.

Nevertheless, simultaneous recording of EEG and fMRI is necessary when the experimental design introduces time-dependent effects such as habituation or learning, or when the brain activity under investigation has, at least, a certain degree of unpredictability. As mentioned earlier, typical examples are abnormal activities in epileptic patients (Salek-Haddadi et al., 2002), sleep stages (Lovblad et al., 1999), and spontaneous fluctuations of different EEG rhythms (Laufs et al., 2003). Also, when the drug modulation of brain responses is investigated (especially in studies involving anaesthetic agents, e.g., Rogers et al., 2004) single, multi-modal recording is advantageous. Lastly, when cognitive or late sensory-evoked potentials need to be explored, the additional sensory stimulation present in a working MR scanner can introduce an important source of difference with the data collected outside, making simultaneous collection desirable; however, the problem reproducibility of cognitive experiments during fMRI acquisition and in a control session is still debated (George et al., 2001). Our results clearly indicate that recording LEPs simultaneously to fMRI does not affect latencies and amplitudes of main waveforms, as well as scalp distribution, and hence suggests the feasibility of combining data from separate, single-modality experiments when the interest is focussed on standard averaged data; this include comparison of results from each modality (locations of LEP sources and fMRI clusters), direct data fusion (constraining the LEP source localization problem with the fMRI clusters), and use of computational neural models (comparing simulated data with experimentally observed values) (Horwitz and Poeppel, 2002). In contrast, when the multi-modal analysis is focussed on single-trial responses to nociceptive stimulation, their intrinsic variability introduces a degree of unpredictability, which imposes the use of simultaneous EEG and fMRI in order to explore the neural activity evoked by the same stimulus. Recording and measuring the same neural response on a trial-by-trial basis with different techniques, besides disclosing relevant physiological information possibly embedded in the between-trial variations, could clarify better the relationship between the nature of the signal measured by EEG and fMRI. For example, the latency jitter of LEPs strongly reduces the amplitude of the average signal as compared to the average of single-trial amplitudes (Iannetti et al., 2005), while it has probably much less impact on the amplitude of the fMRI response because of the intrinsic sluggishness of the hemodynamic response. Furthermore, besides the classical LEP attributes (amplitude and latency), also temporal modulation of EEG power and the phase coherence or resetting relationships induced by single stimuli (a field becoming known as event-related brain dynamics, Makeig et al., 2004) can be compared with the evoked fMRI responses on a single-trial basis. This approach has the potential for developing a new field with the aim of identifying EEG characteristics that correlate most closely with fMRI measures.

Most of the studies recording stimulus-evoked potentials (EPs) and fMRI have adopted an *interleaved* approach, either alternating relatively long periods of fMRI acquisition with similar periods without fMRI scanning (Bonmassar et al., 2001b), or performing "sparse" fMRI, i.e., collecting single images with a delay that allows the registration of the predicted peak of an evoked hemodynamic response (Christmann et al., 2002; Kruggel et al., 2001). In either case, EP recording is carried out during a time window free of RF and gradient switching, thus avoiding the problem of imaging artifact on EEG. Our results show that reliable LEPs can be recorded also when EEG and fMRI are collected at the same time, and this truly simultaneous multi-modal recording avoids the important theoretical and practical limitations of the interleaved approach. First, when long periods of EEG acquisition are interleaved with long periods of fMRI scanning, the two techniques do not sample the same neural phenomenon. Second, even when "sparse" image collection is performed, the hemodynamic response is not sampled in an efficient way (Garreffa et al., 2004; Nebel et al., 2005). Lastly, the interleaved design reduces the flexibility in the stimulus presentation paradigm and increases the overall duration of the experiment, thus augmenting subject discomfort (a particularly important issue in simultaneous EEG/fMRI recording), reducing subject attention and increasing the risk of time-dependent variations of the cognitive state of the subject.

Besides the technical difficulties, it is important to consider that collection of LEPs and fMRI data at the same time has a number of potential confounds related to the nature of EEG and fMRI signals and to the physiology of nociceptive responses. In general, while EEG and fMRI signals are certainly the consequence of spontaneous and stimulus-evoked synaptic activity, the nature of the neural activity they capture is different. LEPs detect time-locked neural activities over a relatively small time window, while fMRI integrates time-locked and non time-locked neural activities. In addition, EEG scalp signals often fail to resolve spatially neural sources overlapping in time, and LEP components, according to the time course of their dipolar sources (e.g., (Schlereth et al., 2003; Valeriani et al., 1996), probably merge neural activity of different cerebral structures (Garcia-Larrea et al., 2003).

The physiological features of the nociceptive system introduce an additional important difference in the way the brain processing of nociceptive input is captured by LEPs and fMRI. While suprathreshold laser stimulation activates concomitantly Aδ and C skin nociceptors and produces the typical dual perception of first, Aδ-mediated, pricking pain followed by a longer-lasting, C-mediated, burning pain, LEPs are present only in the Aδ time window (150–450 ms), without any response in the time window of the C-fibre input (Bromm and Treede, 1984), since cortical EPs primarily reflect changes in sensory input (Garcia-Larrea, 2004; Naatanen and Picton, 1987). In contrast, the different nature of BOLD signal makes fMRI capable to detect slow-rising and longer-lasting sensory stimulation (Bandettini et al., 1997; Porro et al., 1998), and thus it integrates neural processing of both Aδ- and C-fibre input.

Conclusion

Here, we have demonstrated for the first time the feasibility of recording reliable pain-related LEPs and fMRI responses in a truly simultaneous way. We have shown that LEPs recorded during fMRI have very similar characteristics with LEPs recorded outside the magnet with the same experimental paradigm and recording equipment. This finding indicates that multi-modal integration of LEP and fMRI results can be carried out using data collected in separate, single-modality experiments. However, simultaneous collection of LEPs and fMRI now allows analysis

of single-trial responses or experimental designs for paired comparisons of changes during drug modulation or cognitive processes such as memory and learning.

Acknowledgments

This study was partly supported by Pfizer UK Ltd. (GDI, WV), the Saudi Arabian Cultural Bureau in the UK (RKN), the Wellcome Trust (067037/Z/02/Z) (RGW), the Dr. Hadwen Trust for Humane Research (JCWB), the Medical Research Council (FMRIB Centre and PMM) and HEFCE (IT).

References

Allen, P.J., Polizzi, G., Krakow, K., Fish, D.R., Lemieux, L., 1998. Identification of EEG events in the MR scanner: the problem of pulse artifact and a method for its subtraction. NeuroImage 8, 229–239.

Allen, P.J., Josephs, O., Turner, R., 2000. A method for removing imaging artifact from continuous EEG recorded during functional MRI. NeuroImage 12, 230–239.

Bandettini, P.A., Kwong, K.K., Davis, T.L., Tootell, R.B., Wong, E.C., Fox, P.T., Belliveau, J.W., Weisskoff, R.M., Rosen, B.R., 1997. Characterization of cerebral blood oxygenation and flow changes during prolonged brain activation. Hum. Brain Mapp. 5, 93–109.

Baumgartner, C., 2004. Controversies in clinical neurophysiology. MEG is superior to EEG in the localization of interictal epileptiform activity. Con. Clin. Neurophysiol. 115, 1010–1020.

Baumgärtner, U., Cruccu, G., Iannetti, G.D., Treede, R.D., 2005. Laser guns and hot plates. Pain 116 (1–2), 1–3 (Editorial).

Bingel, U., Quante, M., Knab, R., Bromm, B., Weiller, C., Buchel, C., 2003. Single trial fMRI reveals significant contralateral bias in responses to laser pain within thalamus and somatosensory cortices. NeuroImage 18, 740–748.

Bingel, U., Lorenz, J., Glauche, V., Knab, R., Glascher, J., Weiller, C., Buchel, C., 2004. Somatotopic organization of human somatosensory cortices for pain: a single trial fMRI study. NeuroImage 23, 224–232.

Bonmassar, G., Hadjikhani, N., Ives, J.R., Hinton, D., Belliveau, J.W., 2001a. Influence of EEG electrodes on the BOLD fMRI signal. Hum. Brain Mapp. 14, 108–115.

Bonmassar, G., Schwartz, D.P., Liu, A.K., Kwong, K.K., Dale, A.M., Belliveau, J.W., 2001b. Spatiotemporal brain imaging of visual-evoked activity using interleaved EEG and fMRI recordings. NeuroImage 13, 1035–1043.

Bornhovd, K., Quante, M., Glauche, V., Bromm, B., Weiller, C., Buchel, C., 2002. Painful stimuli evoke different stimulus-response functions in the amygdala, prefrontal, insula and somatosensory cortex: a single-trial fMRI study. Brain 125, 1326–1336.

Bromm, B., Treede, R.D., 1984. Nerve fibre discharges, cerebral potentials and sensations induced by CO_2 laser stimulation. Hum. Neurobiol. 3, 33–40.

Bromm, B., Treede, R.D., 1991. Laser-evoked cerebral potentials in the assessment of cutaneous pain sensitivity in normal subjects and patients. Rev. Neurol. (Paris) 147, 625–643.

Buchel, C., Bornhovd, K., Quante, M., Glauche, V., Bromm, B., Weiller, C., 2002. Dissociable neural responses related to pain intensity, stimulus intensity, and stimulus awareness within the anterior cingulate cortex: a parametric single-trial laser functional magnetic resonance imaging study. J. Neurosci. 22 (3), 970–976.

Carmon, A., Friedman, Y., Coger, R., Kenton, B., 1980. Single trial analysis of evoked potentials to noxious thermal stimulation in man. Pain 8, 21–32.

Christmann, C., Ruf, M., Braus, D.F., Flor, H., 2002. Simultaneous electroencephalography and functional magnetic resonance imaging of primary and secondary somatosensory cortex in humans after electrical stimulation. Neurosci. Lett. 333, 69–73.

Churchland, P.S., Sejnowski, T.J., 1988. Perspectives on cognitive neuroscience. Science 242, 741–745.

Collins, D.L., Neelin, P., Peters, T.M., Evans, A.C., 1994. Automatic 3D intersubject registration of MR volumetric data in standardized Talairach space. J. Comput. Assist. Tomogr. 18, 192–205.

Cruccu, G., Pennisi, E., Truini, A., Iannetti, G.D., Romaniello, A., Le Pera, D., De Armas, L., Leandri, M., Manfredi, M., Valeriani, M., 2003. Unmyelinated trigeminal pathways as assessed by laser stimuli in humans. Brain 126, 2246–2256.

Cruccu, G., Anand, P., Attal, N., Garcia-Larrea, L., Haanpaa, M., Jorum, E., Serra, J., Jensen, T.S., 2004. EFNS guidelines on neuropathic pain assessment. Eur. J. Neurol. 11, 153–162.

Czisch, M., Wehrle, R., Kaufmann, C., Wetter, T.C., Holsboer, F., Pollmacher, T., Auer, D.P., 2004. Functional MRI during sleep: BOLD signal decreases and their electrophysiological correlates. Eur. J. Neurosci. 20, 566–574.

Delorme, A., Makeig, S., 2004. EEGLAB: an open source toolbox for analysis of single-trial EEG dynamics including independent component analysis. J. Neurosci. Methods 134, 9–21.

Donaldson, D., Buckner, R., 2001. Effective paradigm design. In: Jezzard, P., Matthews, P.M., Smith, S. (Eds.), Functional MRI. An Introduction to Methods. Oxford Univ. Press, Oxford, pp. 177–195.

Forman, S.D., Cohen, J.D., Fitzgerald, M., Eddy, W.F., Mintun, M.A., Noll, D.C., 1995. Improved assessment of significant activation in functional magnetic resonance imaging (fMRI): use of a cluster-size threshold. Magn. Reson. Med. 33, 636–647.

Frot, M., Mauguière, F., 2003. Dual representation of pain in the operculoinsular cortex in humans. Brain 126, 438–450.

Garcia-Larrea, L., 2004. Somatosensory volleys and cortical evoked potentials: 'first come, first served'? Pain 112, 5–7.

Garcia-Larrea, L., Frot, M., Valeriani, M., 2003. Brain generators of laser-evoked potentials: from dipoles to functional significance. Neurophysiol. Clin. 33, 279–292.

Garreffa, G., Bianciardi, M., Hagberg, G.E., Macaluso, E., Marciani, M.G., Maraviglia, B., Abbafati, M., Carni, M., Bruni, I., Bianchi, L., 2004. Simultaneous EEG-fMRI acquisition: how far is it from being a standardized technique? Magn. Reson. Imaging 22, 1445–1455.

George, J.S., Schmidt, D.M., Rector, D.M., Wood, C., 2001. Dynamic functional neuroimaging integrating multiple modalities. In: Jezzard, P., Matthews, P.M., Smith, S.M. (Eds.), Functional MRI. An Introduction to Methods. Oxford Univ. Press, Oxford, pp. 353–382.

Horwitz, B., Poeppel, D., 2002. How can EEG/MEG and fMRI/PET data be combined? Hum. Brain Mapp. 17, 1–3.

Iannetti, G.D., Truini, A., Galeotti, F., Romaniello, A., Manfredi, M., Cruccu, G., 2001. Usefulness of dorsal laser evoked potentials in patients with spinal cord damage: report of two cases. J. Neurol., Neurosurg. Psychiatry 71, 792–794.

Iannetti, G.D., Truini, A., Romaniello, A., Galeotti, F., Rizzo, C., Manfredi, M., Cruccu, G., 2003. Evidence of a specific spinal pathway for the sense of warmth in humans. J. Neurophysiol. 89, 562–570.

Iannetti, G.D., Leandri, M., Truini, A., Zambreanu, L., Cruccu, G., Tracey, I., 2004. A-delta nociceptor response to laser stimuli: selective effect of stimulus duration on skin temperature, brain potentials and pain perception. Clin. Neurophysiol. 115, 2629–2637.

Iannetti, G.D., Zambreanu, L., Cruccu, G., Tracey, I., 2005. Operculoinsular cortex encodes pain intensity at the earliest stages of cortical processing as indicated by amplitude of laser-evoked potentials in humans. Neuroscience 131, 199–208.

Jenkinson, M., Smith, S., 2001. A global optimisation method for robust affine registration of brain images. Med. Image Anal. 5, 143–156.

Jenkinson, M., Bannister, P., Brady, M., Smith, S., 2002. Improved optimization for the robust and accurate linear registration and motion correction of brain images. NeuroImage 17, 825–841.

Jensen, M.P., Karoly, P., 2001. Self-report scales and procedures for assessing pain in adults. In: Turk, D.C., Melzack, R. (Eds.), Handbook of Pain Assessment. The Guilford Press, New York, pp. 15–34.

Jezzard, P., Clare, S., 2002. fMRI Quality Assurance Procedures. 8th Annual Meeting of the British Chapter of the ISMRM, United Kingdom, pp. 25–26.

Jones, A.K., Brown, W.D., Friston, K.J., Qi, L.Y., Frackowiak, R.S., 1991. Cortical and subcortical localization of response to pain in man using positron emission tomography. Proc. R. Soc. Lond., B Biol. Sci. 244, 39–44.

Krakow, K., Allen, P.J., Symms, M.R., Lemieux, L., Josephs, O., Fish, D.R., 2000. EEG recording during fMRI experiments: image quality. Hum. Brain Mapp. 10, 10–15.

Kruggel, F., Herrmann, C.S., Wiggins, C.J., von Cramon, D.Y., 2001. Hemodynamic and electroencephalographic responses to illusory figures: recording of the evoked potentials during functional MRI. NeuroImage 14, 1327–1336.

Kwong, K.K., Belliveau, J.W., Chesler, D.A., Goldberg, I.E., Weisskoff, R.M., Poncelet, B.P., Kennedy, D.N., Hoppel, B.E., Cohen, M.S., Turner, R., et al., 1992. Dynamic magnetic resonance imaging of human brain activity during primary sensory stimulation. Proc. Natl. Acad. Sci. U. S. A. 89, 5675–5679.

Laufs, H., Kleinschmidt, A., Beyerle, A., Eger, E., Salek-Haddadi, A., Preibisch, C., Krakow, K., 2003. EEG-correlated fMRI of human alpha activity. NeuroImage 19, 1463–1476.

Lemieux, L., Allen, P.J., Franconi, F., Symms, M.R., Fish, D.R., 1997. Recording of EEG during fMRI experiments: patient safety. Magn. Reson. Med. 38, 943–952.

Lemieux, L., Salek-Haddadi, A., Josephs, O., Allen, P., Toms, N., Scott, C., Krakow, K., Turner, R., Fish, D.R., 2001. Event-related fMRI with simultaneous and continuous EEG: description of the method and initial case report. NeuroImage 14, 780–787.

Lenz, F.A., Rios, M., Zirh, A., Chau, D., Krauss, G., Lesser, R.P., 1998. Painful stimuli evoke potentials recorded over the human anterior cingulate gyrus. J. Neurophysiol. 79, 2231–2234.

Lovblad, K.O., Thomas, R., Jakob, P.M., Scammell, T., Bassetti, C., Griswold, M., Ives, J., Matheson, J., Edelman, R.R., Warach, S., 1999. Silent functional magnetic resonance imaging demonstrates focal activation in rapid eye movement sleep. Neurology 53, 2193–2195.

Makeig, S., Debener, S., Onton, J., Delorme, A., 2004. Mining event-related brain dynamics. Trends Cogn. Sci. 8, 204–210.

Menon, R.S., Goodyear, B.G., 2001. Spatial and temporal resolution in fMRI. In: Jezzard, P., Matthews, P.M., Smith, S.M. (Eds.), Functional MRI An Introduction to Methods. Oxford Univ. Press, Oxford, pp. 145–158.

Michel, C.M., Murray, M.M., Lantz, G., Gonzalez, S., Spinelli, L., Grave de Peralta, R., 2004. EEG source imaging. Clin. Neurophysiol. 115, 2195–2222.

Naatanen, R., Picton, T., 1987. The N1 wave of the human electric and magnetic response to sound: a review and an analysis of the component structure. Psychophysiology 24, 375–425.

Nebel, K., Stude, P., Wiese, H., Muller, B., de Greiff, A., Forsting, M., Diener, H.C., Keidel, M., 2005. Sparse imaging and continuous event-related fMRI in the visual domain: a systematic comparison. Hum. Brain Mapp. 24, 130–143.

Niazy, R.K.N., Beckmann, C.B., Iannetti, G.D., Brady, J.M., Smith, S., this issue. Removal of fMRI-environment artifacts from EEG data using optimal basis sets. NeuroImage. doi:10.1016/j.neuroimage.2005.06.067.

Ogawa, S., Tank, D.W., Menon, R., Ellermann, J.M., Kim, S.G., Merkle, H., Ugurbil, K., 1992. Intrinsic signal changes accompanying sensory stimulation: functional brain mapping with magnetic resonance imaging. Proc. Natl. Acad. Sci. U. S. A. 89, 5951–5955.

Ohara, S., Crone, N.E., Weiss, N., Treede, R.D., Lenz, F.A., 2004. Cutaneous painful laser stimuli evoke responses recorded directly from primary somatosensory cortex in awake humans. J. Neurophysiol. 91, 2734–2746.

Peyron, R., Laurent, B., Garcia-Larrea, L., 2000. Functional imaging of brain responses to pain. A review and meta-analysis. Neurophysiol. Clin. 30, 263–288.

Porro, C.A., Cettolo, V., Francescato, M.P., Baraldi, P., 1998. Temporal and intensity coding of pain in human cortex. J. Neurophysiol. 80, 3312–3320.

Rogers, R., Wise, R.G., Painter, D.J., Longe, S.E., Tracey, I., 2004. An investigation to dissociate the analgesic and anesthetic properties of ketamine using functional magnetic resonance imaging. Anesthesiology 100, 292–301.

Salek-Haddadi, A., Merschhemke, M., Lemieux, L., Fish, D.R., 2002. Simultaneous EEG-correlated ictal fMRI. NeuroImage 16, 32–40.

Sawamoto, N., Honda, M., Okada, T., Hanakawa, T., Kanda, M., Fukuyama, H., Konishi, J., Shibasaki, H., 2000. Expectation of pain enhances responses to nonpainful somatosensory stimulation in the anterior cingulate cortex and parietal operculum/posterior insula: an event-related functional magnetic resonance imaging study. J. Neurosci. 20, 7438–7445.

Schlereth, T., Baumgartner, U., Magerl, W., Stoeter, P., Treede, R.D., 2003. Left-hemisphere dominance in early nociceptive processing in the human parasylvian cortex. NeuroImage 20, 441–454.

Speckmann, E., Elger, C., 1999. Introduction to the neurophysiological basis of the EEG and DC potentials. In: Niedermeyer, E., Lopes Da Silva, F. (Eds.), Electroencephalography. Basic Principles, Clinical Applications, and Related Fields. Lippincott Williams and Wilkins, Baltimore, pp. 15–27.

Spiegel, J., Hansen, C., Treede, R.D., 2000. Clinical evaluation criteria for the assessment of impaired pain sensitivity by thulium-laser evoked potentials. Clin. Neurophysiol. 111, 725–735.

Spiegel, J., Hansen, C., Baumgartner, U., Hopf, H.C., Treede, R.D., 2003. Sensitivity of laser-evoked potentials versus somatosensory evoked potentials in patients with multiple sclerosis. Clin. Neurophysiol. 114, 992–1002.

Tarkka, I.M., Treede, R.D., 1993. Equivalent electrical source analysis of pain-related somatosensory evoked potentials elicited by a CO_2 laser. J. Clin. Neurophysiol. 10, 513–519.

Towell, A.D., Boyd, S.G., 1993. Sensory and cognitive components of the CO_2 laser evoked cerebral potential. Electroencephalogr. Clin. Neurophysiol. 88, 237–239.

Tracey, I., Ploghaus, A., Gati, J.S., Clare, S., Smith, S., Menon, R.S., Matthews, P.M., 2002. Imaging attentional modulation of pain in the periaqueductal gray in humans. J. Neurosci. 22, 2748–2752.

Treede, R.D., Meyer, R.A., Raja, S.N., Campbell, J.N., 1995. Evidence for two different heat transduction mechanisms in nociceptive primary afferents innervating monkey skin. J. Physiol. 483 (Pt. 3), 747–758.

Valeriani, M., Rambaud, L., Mauguière, F., 1996. Scalp topography and dipolar source modelling of potentials evoked by CO_2 laser stimulation of the hand. Electroencephalogr. Clin. Neurophysiol., 343–353.

Vogel, H., Port, J.D., Lenz, F.A., Solaiyappan, M., Krauss, G., Treede, R.D., 2003. Dipole source analysis of laser-evoked subdural potentials recorded from parasylvian cortex in humans. J. Neurophysiol. 89, 3051–3060.

Woolrich, M.W., Ripley, B.D., Brady, M., Smith, S.M., 2001. Temporal autocorrelation in univariate linear modeling of fMRI data. NeuroImage 14, 1370–1386.

Worsley, K.J., Friston, K.J., 1995. Analysis of fMRI time-series revisited—Again. NeuroImage 2, 173–181.

Worsley, K.J., Evans, A.C., Marrett, S., Neelin, P., 1992. A three-dimensional statistical analysis for CBF activation studies in human brain. J. Cereb. Blood Flow Metab. 12, 900–918.

Youell, P.D., Wise, R.G., Bentley, D.E., Dickinson, M.R., King, T.A., Tracey, I., Jones, A.K., 2004. Lateralisation of nociceptive processing in the human brain: a functional magnetic resonance imaging study. NeuroImage 23, 1068–1077.